Hindawi
Contrast Media & Molecular Imaging
Volume 2021, Article ID 6347404, 8 pages
https://doi.org/10.1155/2021/6347404

Research Article

Radiomic Features of ^{18}F-FDG PET in Hodgkin Lymphoma Are Predictive of Outcomes

Yeye Zhou,[1] **Yuchun Zhu**,[2] **Zhiqiang Chen**,[1] **Jihui Li**,[1] **Shibiao Sang**,[1] **and Shengming Deng**[1,3,4]

[1]*Department of Nuclear Medicine, The First Affiliated Hospital of Soochow University, Suzhou, China*
[2]*Department of Nuclear Medicine, First People's Hospital of Kunshan, Kunshan, China*
[3]*Nuclear Medicine Laboratory of Mianyang Central Hospital, Mianyang 621099, China*
[4]*State Key Laboratory of Radiation Medicine and Protection, Soochow University, Suzhou,215123, China*

Correspondence should be addressed to Shibiao Sang; sshibiao@163.com and Shengming Deng; dshming@163.com

Received 16 August 2021; Revised 10 October 2021; Accepted 28 October 2021; Published 22 November 2021

Academic Editor: Reza Vali

Purpose. In the present study, we aimed to investigate whether the radiomic features of baseline ^{18}F-FDG PET can predict the prognosis of Hodgkin lymphoma (HL). *Methods*. A total 65 HL patients (training cohort: $n = 49$; validation cohort: $n = 16$) were retrospectively enrolled in the present study. A total of 47 radiomic features were extracted from pretreatment PET images. The least absolute shrinkage and selection operator (LASSO) regression was used to select the most useful prognostic features in the training cohort. The distance between the two lesions that were the furthest apart (D_{max}) was recorded. The receiver operating characteristic (ROC) curve, Kaplan–Meier method, and Cox proportional hazards model were used to assess the prognostic factors. *Results*. Long-zone high gray-level emphasis extracted from a gray-level zone-length matrix ($LZHGE_{GLZLM}$) (HR = 9.007; $p = 0.044$) and Dmax (HR = 3.641; $p = 0.048$) were independently correlated with 2-year progression-free survival (PFS). A prognostic stratification model was established based on both risk predictors, which could distinguish three risk categories for PFS ($p = 0.0002$). The 2-year PFS was 100.0%, 64.7%, and 33.3%, respectively. *Conclusions*. $LZHGE_{GLZLM}$ and Dmax were independent prognostic factors for survival outcomes. Besides, we proposed a prognostic stratification model that could further improve the risk stratification of HL patients.

1. Introduction

Hodgkin lymphoma (HL) is a hematological malignancy, with an excellent prognosis for most patients [1]. However, a small number of patients still suffer from relapsed or refractory disease, and their prognosis is poor [2, 3]. The currently available prognostic indicators fail to identify high-risk patients [4, 5]. Therefore, it is urgently necessary to identify patients with a low or high risk of recurrence [6].

A combination of functional-metabolic and morphological imaging and 18F-fluorodeoxyglucose positron emission tomography/computed tomography (^{18}F-FDG PET/CT) has become a standard imaging modality for HL patients [7–9]. Recently, a simple imaging feature measured on baseline ^{18}F-FDG PET/CT can be useful in reflecting lesion dissemination of patients with lymphoma [10]. A high Dmax is associated with a poor prognosis [11].

Radiomics is an emerging field that converts digital imaging data into a high-dimensional mineable feature space using high-throughput computing [12, 13]. By extracting a large number of quantitative features from tomographic images, radiomics has the potential to allow the assessment of tumor heterogeneity, which maybe correlated with clinical outcomes (Figure 1) [14–16]. Recent studies have reported the feasibility of radiomics in the prognosis of patients with various malignancies [15–18]. However, research using radiomics nomograms based on ^{18}F-FDG PET for HL is relatively limited.

We, therefore, aimed to evaluate whether radiomic features derived from pretreatment ^{18}F-FDG PET imaging

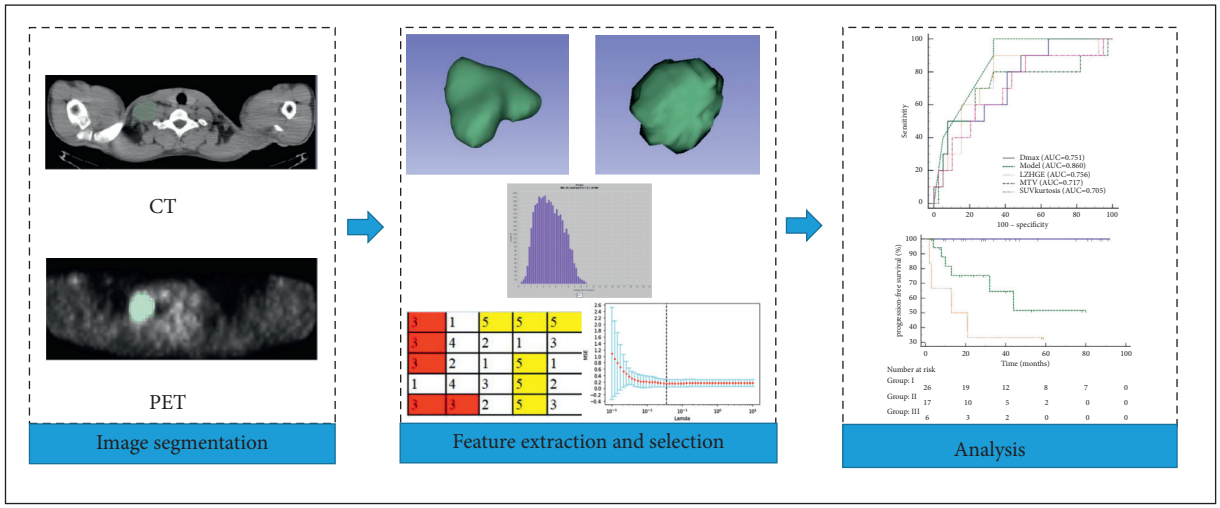

FIGURE 1: Workflow of the radiomics analysis. A 22-year-old man underwent ^{18}F-FDG PET/CT for staging work-up of Hodgkin lymphoma (nodular sclerosis) with a maximum SUV of 10.95. The volume of interest (VOI) of the lymphoma lesion was manually delineated. 41% of SUV_{max} was applied as a threshold to optimize the VOI. The patient did not show progression and survived at the end of the 17-month follow-up period.

could predict progression-free survival (PFS), alone or in combination with other parameters.

2. Materials and Methods

2.1. Patients. This retrospective study was approved by the institutional review board of the First Affiliated Hospital of Soochow University, and informed consent was waived. This study was carried out following the Declaration of Helsinki with a trial registration number of ChiCTR2100045957. All HL patients diagnosed from March 2013 to December 2020 were included in the present study. The inclusion criteria were set as follows: (1) histologically confirmed HL and (2) no chemo- or radiotherapy treatment before ^{18}F-FDG PET/CT examination. Patients with other types of cancers or with incomplete clinical and imaging datasets were excluded.

A total of 65 patients (45 males and 20 females, mean age: 29 years, age range: 8–72 years) were randomly divided into the training ($n = 49$) and validation ($n = 16$) cohorts following a ratio of 7 : 3 [12, 19]. Clinicopathological data for each HL patient, including gender, age, B symptoms, level, Ann Arbor stage, bone marrow (BM) biopsy, bulky disease (>10 cm), D_{max}, and PET/CT imaging data were acquired.

2.2. PET/CT Acquisition. All patients were asked not to eat for at least 6 h before the administration of ^{18}F-FDG (4.07–5.55 MBq/kg). Blood glucose levels were less than 11 mmol/L. A whole-body scan was acquired at 60 ± 10 min after intravenous injection of ^{18}F-FDG using an integrated PET/CT scanner (Discovery STE; General Electric Medical Systems, Milwaukee WI, USA). First, low-dose CT images were performed, with parameters as follows: 140 kV, 120 mA, a transaxial FOV of 70 cm, a pitch of 1.75, a rotation time of 0.8 s, and a slice thickness of 3.75 mm, followed by PET images, with 2-3 min per bed position and 7-8 bed position per patient.

2.3. Feature Extraction and Selection. The radiomic features were extracted from PET images using LIFEx freeware (v6.30 https://www.lifexsoft.org/) [20]. PET and CT images of the DICOM format were transferred to LIFEx freeware and automatically fused by the freeware. Areas with increased uptake of ^{18}F-FDG on PET and abnormal density on CT were defined as lesions. The volume of interest (VOI) of the lymphoma lesion was manually delineated slice by slice using three-dimensional drawing tools by two experienced nuclear medicine physicians. Moreover, 41% of the maximum standardized uptake value (SUV_{max}) was applied as a threshold to optimize the VOI [21]. Spatial resampling was 2 × 2 × 2 mm voxel size. Intensity discretization for PET data was processed with the number of gray levels of 64 bins and absolute scale bounds between 0 and 20 [22, 23]. After preprocessing, a total of 47 radiomic features were extracted from PET images, including conventional imaging parameters, histogram (HISTO), shape, gray-level co-occurrence matrix (GLCM), gray-level run-length matrix (GLRLM), neighborhood gray-level different matrix (NGLDM), and gray-level zone-length matrix (GLZLM) (Table 1).

A total of 15 patients were randomly selected to calculate the interobserver agreement of the feature extraction. The intraclass correlation coefficient (ICC) was used to determine the repeatability/reproducibility of features in our research, and ICC >0.75 was selected [24–26]. Subsequently, the least absolute shrinkage and selection operator (LASSO) COX regression model was used to select the most useful prognostic features with 10-fold cross validation for selecting the parameter Lambda in the training cohort [27, 28].

2.4. Treatment and Follow-Up. Patients were treated according to the institution's standard protocol. A total of 19 patients with early-stage disease (stage I and II without risk factors) were generally treated with an ABVD regimen

Table 1: Radiomic parameters.

Index	Matrix	Parameter
Conventional		SUV_{min}, SUV_{mean}, SUV_{max}, SUV_{peak}, and SUV_{Std}
Advanced indices		MTV and TLG
Histogram-derived parameters		Skewness, kurtosis, entropy, and energy
Shape-derived parameters		Sphericity and compacity
Texture features	GLCM	Homogeneity, energy, contrast, correlation, entropy, and dissimilarity
	GLRLM	SRE/LRE, LGRE/HGRE, SRLGE/SRHGE, LRLGE/LRHGE, GLNU/RLNU, and RP
	NGLDM	Coarseness, contrast, and busyness
	GLZLM	SZE, LZE, LGZE, HGZE, SZLGE, SZHGE, LZLGE, LZHGE, GLNU, ZLNU, and ZP

MTV: metabolic tumor volume; TLG: total lesion glycolysis; GLCM: gray-level co-occurrence matrix; GLRLM: gray-level run-length matrix; SRE/LRE: short/long-run emphasis; LGRE/HGRE: low/high gray-level run emphasis; SRLGE/SRHGE: short-run low/high gray-level emphasis; LRLGE/LRHGE: long-run low/high gray-level emphasis; GLNU/RLNU: gray-level nonuniformity/run-length nonuniformity; RP: run percentage; NGLDM: neighborhood gray-level difference matrix; GLZLM: gray-level zone-length matrix; SZE/LZE: short/long-zone emphasis; LGZE/HGZE: low/high gray-level zone emphasis; SZLGE/SZHGE: short-zone low/high gray-level emphasis; LZLGE/LZHGE: long-zone low/high gray-level emphasis; GLNU/ZLNU: gray-level nonuniformity or zone-length nonuniformity; ZP; zone percentage.

(adriamycin, bleomycin, vinblastine, and dacarbazine). Moreover, 18 intermediate-stage patients generally received 4 to 6 cycles of ABVD, followed by involved-field radiotherapy. In addition, 31 advanced-stage patients (stage III and IV) were generally treated with 6 to 8 cycles of ABVD alone or a combination of chemotherapy and radiotherapy. Four patients received autologous stem cell transplantation after relapse. Patients were followed up by routine imaging methods (MRI, CT, or ^{18}F-FDG PET/CT) every 3 months during the first 2 years and every 6 months thereafter. To allow earlier individual treatment, the PFS was set as the main endpoint [29].

2.5. Statistical Analysis. Statistical analyses were performed using SPSS software version 26.0 (SPSS Inc., Chicago, IL, USA) and python 3.0 (https://www.python.org). The differences in patients' characteristics between the training and validation cohorts were compared using the Chi-square test. The cutoff value of the radiomic features was defined by the receiver operating characteristic (ROC) curve according to Youden's index. The Kaplan–Meier method and log-rank test were used to estimate PFS. Multivariate analyses were performed using the Cox proportional hazards model. A $p < 0.05$ was considered statistically significant. The distances between all pairs of lesions (including both nodal and extranodal lesions) were calculated using the LIFEx software [20].

3. Results

3.1. Patient Characteristics. Table 2 summarizes the clinical and PET characteristics of patients in the training and validation cohorts. A total of 65 patients were enrolled in this study. Of these patients, 31 patients presented with nodular sclerosis, 14 patients presented with mixed cellularity, four patients presented as lymphocyte rich, two patients presented with lymphocyte depletion, and 14 patients presented with nodular lymphocyte-predominant subtypes. The relapse or progression of disease occurred in 14 patients (21.5%) with a median time of 11 months (range of 2–57 months). The median PFS was 40 months (range of 2–92 months). No significant differences were found between the two cohorts ($p = 0.389$–0.703).

3.2. Feature Selection in the Training Cohort. A total of 47 radiomic features were extracted in the training dataset. Based on the LASSO results, metabolic tumor volume (MTV), SUV kurtosis, and long-zone high gray-level emphasis extracted from the gray-level zone-length matrix ($LZHGE_{GLZLM}$) were selected as potential prognostic factors for PFS. From ROC curves, the cutoff value of MTV was 135 cm^3, SUV kurtosis was 5.6, and $LZHGE_{GLZLM}$ was 3,200 (Figure 2). The ICC of the three radiomic features was 0.94, 0.80, and 0.84, respectively.

3.3. Univariate and Multivariate Analyses. Table 3 shows the results of univariate and multivariate analyses of the clinical parameters and PET variables that can discriminate different survival endpoints. The optimal cutoff value for D_{max} was 57.4 with an AUC of 0.751. In the univariate analysis, the BM biopsy, D_{max}, MTV, SUV kurtosis, and $LZHGE_{GLZLM}$ of radiomic features were associated with PFS. These variables were input into the multivariate Cox analysis. After multivariate analysis, $LZHGE_{GLZLM}$ (HR = 9.007; $p = 0.044$) and Dmax (HR = 3.641; $p = 0.048$) remained prognostic factors for PFS.

High Dmax (>57.4 cm) and $LZHGE_{GLZLM}$ (>3,200) were significantly associated with a shorter PFS (Figure 3). Patients with high Dmax had a 2-year PFS of 42.9%, whereas patients with low Dmax had a 2-year PFS of 90.5% ($p = 0.0002$). Moreover, patients with high $LZHGE_{GLZLM}$ had a 2-year PFS of 63.6%, whereas patients with low $LZHGE_{GLZLM}$ had a 2-year PFS of 100.0% ($p = 0.0013$).

3.4. Combination of Radiomic and Dissemination Features. A prognostic stratification model was established based on the independent risk factors (Dmax and$LZHGE_{GLZLM}$) presented in the multivariate analysis for PFS. Therefore, three risk categories could be significantly distinguished ($p = 0.0002$) (Figure 4), including group I with no risk factors ($n = 26$); group II with one risk factor only ($n = 17$); and group III with two risk factors ($n = 6$), and the PFS of the

Table 2: Characteristics of the training and validation cohorts.

	Total ($n = 65$)	Training ($n = 49$)	Validation ($n = 16$)	p
Sex				
Male	45 (69.2%)	34 (69.4%)	11 (68.8%)	0.596
Female	20 (30.8%)	15 (30.6%)	5 (31.3%)	
Age, median (range)	29.0 (8–72)	29 (8–72)	30 (16–54)	0.703
Ann Arbor stage				
I-II	36 (55.4%)	27 (55.1%)	9 (56.3%)	0.585
III-IV	29 (44.6%)	22 (44.9%)	7 (43.8%)	
Bulky disease				
>10 cm	9 (13.8%)	6 (12.2%)	3 (18.8%)	0.678
<10 cm	56 (86.2%)	43 (87.8%)	13 (81.3%)	
BM				
Yes	9 (13.8%)	7 (14.3%)	2 (12.5%)	0.612
No	56 (86.2%)	42 (85.7%)	14 (87.5%)	
Extranodal sites				
Yes	25 (38.5%)	20 (40.8%)	5 (31.3%)	0.495
No	40 (61.5%)	29 (59.2%)	11 (68.8%)	
B symptoms				
Yes	22 (33.8%)	18 (36.7%)	4 (25.0%)	0.389
No	43 (66.2%)	31 (63.3%)	12 (75.0%)	
Chemotherapy with IFRT				
Yes	4 (6.2%)	4 (8.2%)	0 (0.0%)	0.565
No	61 (93.8%)	45 (91.8%)	16 (100.0%)	

LDH, lactate dehydrogenase, BM, bone marrow; IFRT, involved-field radiation therapy.

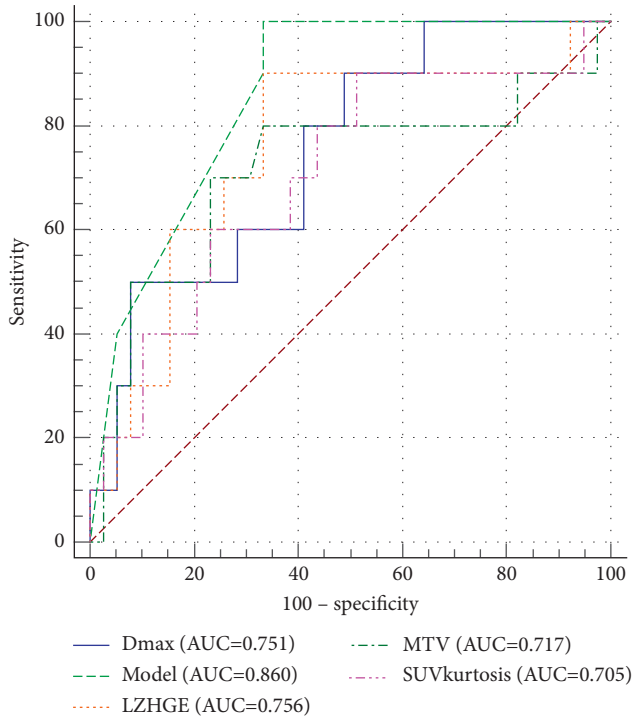

Figure 2: ROC curves and area under the curve (AUC) values of the radiomic features.

abovementioned three groups was 100.0%, 64.7%, and 33.3% ($p = 0.0002$), respectively. Comparison between group I and group II or between group I and group III revealed significantly different PFS ($p = 0.001$, $p < 0.0001$, respectively), whereas comparison between group II and group III did not reach statistical significance ($p = 0.205$).

4. Discussion

The present study demonstrated that ^{18}F-FDG PET radiomic signature was useful for predicting survival outcomes in HL patients, and $LZHGE_{GLZLM}$ and D_{max} were independent prognostic factors for PFS. Moreover, we established a prognostic stratification model based on two radiomic features, and HL patients were divided into three risk groups. The results indicated that PET radiomics might be helpful for prognostic evaluation of HL patients.

Intratumor heterogeneity is a recognized feature of malignancy, reflecting areas of high cell density, hypoxia, angiogenesis, and necrosis [30, 31]. It is a pivotal dimension associated with tumor aggressiveness and patient outcomes [32, 33]. Radiomics analysis of noninvasive imaging is a widely used approach to quantify intratumor heterogeneity [34]. Previous studies have shown that textural features can effectively predict treatment response and patient survival for various types of cancer [30, 35, 36]. Our results indicated that SUV kurtosis and $LZHGE_{GLZLM}$ might improve the risk stratification in HL patients. Specifically, $LZHGE_{GLZLM}$ was significantly related to PFS after multivariate analysis. Both radiomic features implied the measurement of intratumor heterogeneity. Kurtosis reflects the peak or flatness of an SUV intensity-volume histogram, and it is increased with higher heterogeneity [37]. $LZHGE_{GLZLM}$ represents the distribution of the long homogeneous zones with high gray levels. A higher $LZHGE_{GLZLM}$ is associated with a poor PFS.

Table 3: Univariate and multivariate analyses for prognostic factors of PFS.

	Features	p value	HR (95% CI)
Univariate analysis			
Clinical parameters	Gender	0.1726	2.579 (0.6609–10.06)
	Age (>30)	0.2104	0.4514 (0.1300–1.567)
	Ann Arbor stage	0.0590	3.394 (0.9548–12.07)
	Extranodal sites	0.1788	2.398 (0.6700–8.581)
	B symptoms	0.2791	2.067 (0.5550–7.698)
	BM	0.0213*	9.985 (1.363–46.78)
	Bulky disease (>10 cm)	0.2886	3.078 (0.3859–24.55)
	D_{max}	0.0002*	34.78 (5.206–232.4)
	Chemotherapy with IFRT	0.0908	8.589 (0.7105–103.8)
PET variables	SUVmax	0.0723	10.52 (0.8081–137.0)
	MTV	0.0016*	9.811 (2.371–40.59)
	SUV kurtosis	0.0316*	3.961 (1.129–13.90)
	$LZHGE_{GLZLM}$	0.0013*	8.036 (2.258–28.60)
Multivariable analysis			
	BM	0.086	—
	D_{max}	0.048*	3.641 (1.011–13.110)
	MTV	0.618	—
	SUV kurtosis	0.243	—
	$LZHGE_{GLZLM}$	0.044*	9.007 (1.066–76.116)

*Statistically significant. HR, hazard ratio; CI, confidence interval; LDH, lactate dehydrogenase; BM, bone marrow; D_{max}, the distance between the two lesions that were the furthest apart; MTV, metabolic tumor volume; LZHGE, long-zone high gray-level emphasis; GLZLM, gray-level zone-length matrix.

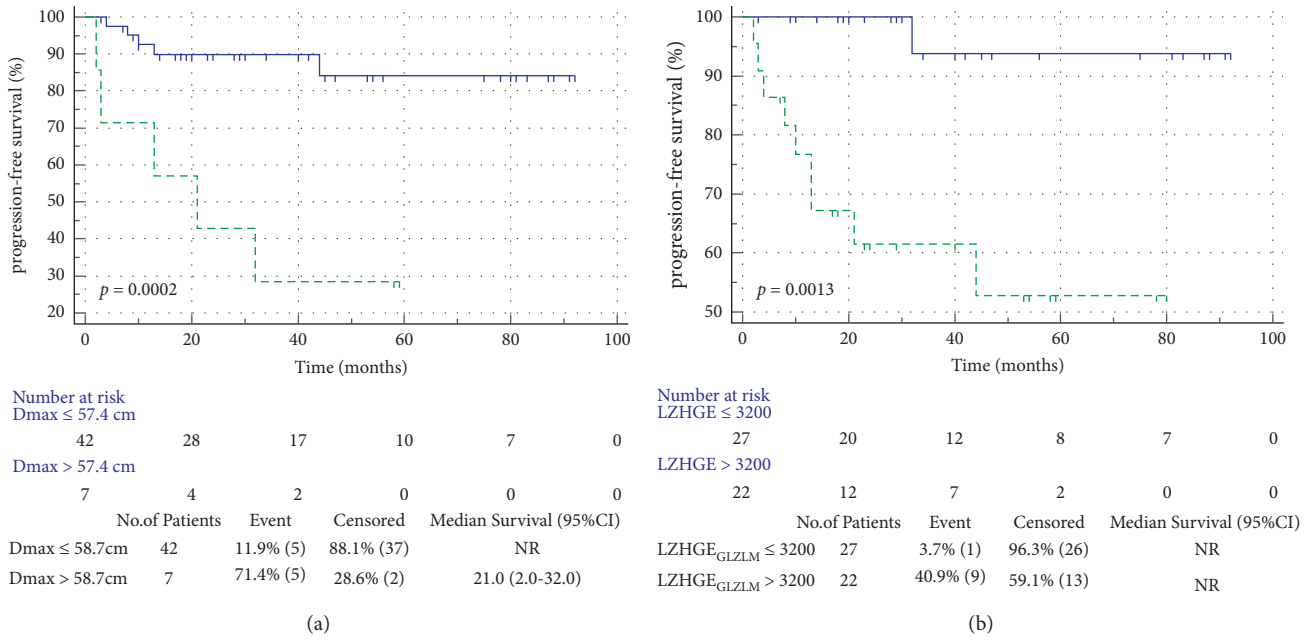

Figure 3: Kaplan–Meier survival analysis of PFS according to D_{max} (a) and $LZHGE_{GLZLM}$ (b). NR, not reached.

At present, few studies have investigated the role of PET radiomics in predicting treatment outcomes in HL. Lue et al. [14] have found that SUV kurtosis is significantly related to PFS, and INU_{GLRM} is significantly associated with PFS and overall survival (OS). Another study has reported that wavelet HIR_GLRMPET and RLNU_GLRMCT are independent predictive factors for treatment response. The INU_GLRMPET and wavelet SRE_GLRMCT are associated with PFS, whereas ZSNU_GLSZMPET is a prognostic factor for OS [38]. Our findings were consistent with the above-mentioned studies, indicating that PET radiomic features were useful for prognostic evaluation of HL patients.

Traditional PET metabolic parameters, such as MTV, have been proved to be significant prognostic indicators for the prognosis of HL patients [39, 40]. Parvez et al. have reported that the MTV can predict the response after therapy in 82 patients with aggressive B-cell lymphoma, while textural features cannot predict the treatment

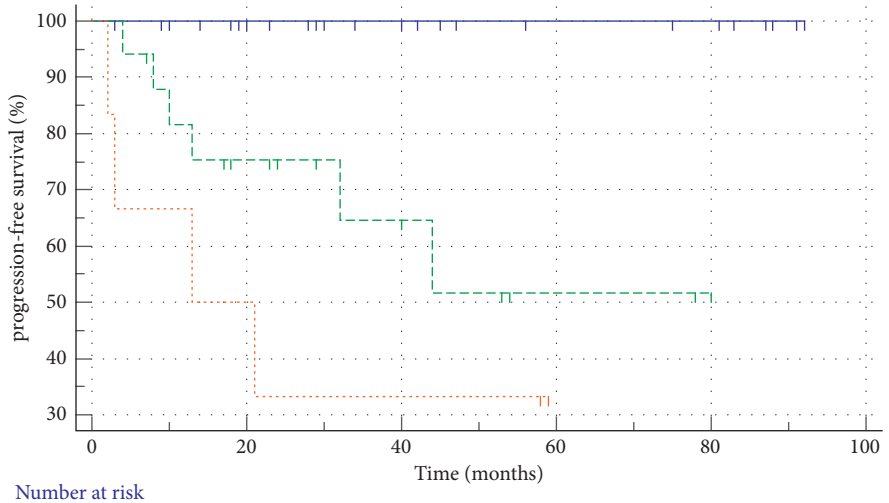

Number at risk

Group: I					
26	19	12	8	7	0
Group: II					
17	10	5	2	0	0
Group: III					
6	3	2	0	0	0

	No.of Patients	Event	Censored	Median Survival (95%CI)
Low $LZHGE_{GLZLM}$ and Low Dmax	26	0.0% (0)	100.0% (27)	NR
High $LZHGE_{GLZLM}$ or High Dmax	17	35.3% (6)	64.7% (10)	NR
High $LZHGE_{GLZLM}$ and High Dmax	6	66.7% (4)	33.3% (3)	13.0 (2.0-21.0)

Figure 4: PFS according to $LZHGE_{GLZLM} \leq 3{,}200$ and $D_{max} \leq 57.4$ cm, $LZHGE_{GLZLM} > 3{,}200$ and $D_{max} > 57.4$ cm, and $LZHGE_{GLZLM} > 3{,}200$ and $D_{max} > 58.7$ cm. NR, not reached.

response, although several features are related to residual mass and outcomes [41]. However, several reports have demonstrated that the intratumor heterogeneity for survival prognostication is superior to traditional PET metabolic parameters [38, 42, 43]. Lue et al. have revealed that the pretreatment intensity nonuniformity of ^{18}F-FDG PET is a promising prognostic indicator in HL patients and may outperform MTV [14]. In our present study, MTV was associated with PFS in the univariate analysis, while MTV did not retain the prognostic significance in the multivariate analysis. Many sources may cause these differences, such as small sample size, image segmentation, acquisition and reconstruction parameters, and feature extraction software [44]. Further investigations in a larger cohort population are required to validate our conclusions.

To the best of our knowledge, we, for the first time, predicted the survival outcomes of HL patients using the D_{max} feature. D_{max}, which is the largest distance between all pairs of lesions, captures the spread of the disease. Recently, an analysis consisting of 95 patients with advanced-stage diffuse large B-cell lymphoma has reported that D_{max} is an independent predictor of PFS and OS. A high D_{max} was associated with an adverse prognosis, suggesting that the measurement of tumor dissemination was an essential biomarker for patients with lymphoma. The combination of PET radiomic features and D_{max} makes it possible to identify patients with a poor prognosis and guide clinicians to change treatment regimens [10]. In our present study, D_{max} was an independent prognostic factor of PFS, and the 2-year PFS in the high D_{max} and low D_{max} groups was 42.9% and 90.5%, respectively. Additionally, we established a prognostic stratification model based on Dmax and imaging features ($LZHGE_{GLZLM}$) that predicted survival outcomes of HL patients. Indeed, patients with high D_{max} (>57.4 cm) and high $LZHGE_{GLZLM}$ (>3,200) had a much worse prognosis compared with the other patients. The new model successfully improved patient risk stratification.

Repeatability and robustness are crucial in radiomics analysis [45]. In the present study, all ^{18}F-FDG PET/CT images were realized in the same center using the same acquisition and reconstruction protocols. To reduce the impact of discretization values on robustness, a reliable discretization using a fixed size of bins was adopted [46]. Furthermore, our investigation of interobserver variability and LASSO logistic with 10-fold cross validation supported the robustness and prognostic power of the identified imaging features. Further external analysis of our results in a larger cohort is necessary and promotes the clinical application of radiomic features.

The present study has several limitations. First, this was a single-center retrospective study, and potential selection bias might exist. Second, the sample size was relatively small in

the training cohort, particularly for the identification of available features in texture analysis. Besides, the interobserver variability could be affected by different image readers. Consequently, large-scale multicenter studies of the risk model are required to further verify its value.

5. Conclusions

Our results indicated the association between pretreatment ^{18}F-FDG PET radiomic features and relapsed disease status in HL patients. Besides, a prognostic scoring system consisting of the Dmax and $LZHGE_{GLZLM}$ could be useful to improve risk stratification, which might be beneficial for personalized treatment.

Data Availability

The patient data used to support the findings of this study are available from the corresponding author upon request.

Disclosure

Yeye Zhou, Yuchun Zhu, Zhiqiang Chen, and Jihui Li are the co-first authors.

Conflicts of Interest

The authors declare no conflicts of interest.

Authors' Contributions

Yeye Zhou, Yuchun Zhu, Zhiqiang Chen, and Jihui Li contributed equally to this article.

Acknowledgments

The present study was supported by the National Natural Science Foundation of China (grant no. 81601522), Medical Youth Talent Project of Jiangsu Province (grant no. QNRC2016749), Gusu Health Talent Program (grant no. GSWS2020013), Suzhou People's Livelihood Science and Technology Project (grant no. SYS2019038), Project of State Key Laboratory of Radiation Medicine and Protection, Soochow University (No. GZK1202127), and the Open Foundation of Nuclear Medicine Laboratory of Mianyang Central Hospital, (Nos. 2021HYX023, 2021HYX026, and 2021HYX029).

References

[1] M. P. E. André, T. Girinsky, and M. Federico, "Early positron emission tomography response–adapted treatment in stage I and II Hodgkin lymphoma: final results of the randomized EORTC/LYSA/FIL H10 trial," *Journal of Clinical Oncology*, vol. 35, no. 16, pp. 1786–1794, 2017.

[2] N. W. Ozuah and A. S. Lacasce, "Clinical evaluation and management of Hodgkin lymphoma," in *Concise Guide to Hematology*Springer, Berlin, Germany, 2019.

[3] S. M. Ansell, "Hodgkin lymphoma: 2018 update on diagnosis, risk-stratification, and management," *American Journal of Hematology*, vol. 93, no. 5, pp. 704–715, 2018.

[4] D. Hasenclever, V. Diehl, J. O. Armitage et al., "A prognostic score for advanced hodgkin's disease," *New England Journal of Medicine*, vol. 339, no. 21, pp. 1506–1514, 1998.

[5] S. Kanoun, C. Rossi, A. Berriolo-Riedinger et al., "Baseline metabolic tumour volume is an independent prognostic factor in Hodgkin lymphoma," *European Journal of Nuclear Medicine and Molecular Imaging*, vol. 41, no. 9, pp. 1735–1743, 2014.

[6] R. Frood, C. Burton, C. Tsoumpas et al., "Baseline PET/CT imaging parameters for prediction of treatment outcome in Hodgkin and diffuse large B cell lymphoma: a systematic review," *European Journal of Nuclear Medicine and Molecular Imaging*, vol. 48, no. 10, pp. 3198–3220, 2021.

[7] S. Kanoun, C. Rossi, and O. Casasnovas, "[18F] FDG-PET/CT in Hodgkin lymphoma: current usefulness and perspectives," *Cancers*, vol. 10, no. 5, 2018.

[8] B. D. Cheson, R. I. Fisher, S. F. Barrington et al., "Recommendations for initial evaluation, staging, and response assessment of Hodgkin and non-hodgkin lymphoma: the lugano classification," *Journal of Clinical Oncology*, vol. 32, no. 27, pp. 3059–3067, 2014.

[9] J. M. Zaucha, S. Chauvie, R. Zaucha, A. Biggii, and A. Gallamini, "The role of PET/CT in the modern treatment of Hodgkin lymphoma," *Cancer Treatment Reviews*, vol. 77, pp. 44–56, 2019.

[10] A.-S. Cottereau, C. Nioche, A.-S. Dirand et al., "18F-FDG PET dissemination features in diffuse large B-cell lymphoma are predictive of outcome," *Journal of Nuclear Medicine*, vol. 61, no. 1, pp. 40–45, 2020.

[11] A.-S. Cottereau, M. Meignan, C. Nioche et al., "Risk stratification in diffuse large B-cell lymphoma using lesion dissemination and metabolic tumor burden calculated from baseline PET/CT†," *Annals of Oncology*, vol. 32, no. 3, pp. 404–411, 2021.

[12] R. J. Gillies, P. E. Kinahan, and H. Hricak, "Radiomics: images are more than pictures, they are data," *Radiology*, vol. 278, no. 2, pp. 563–577, 2016.

[13] H. J. Aerts, E. R. Velazquez, R. T. Leijenaar et al., "Decoding tumour phenotype by noninvasive imaging using a quantitative radiomics approach," *Nature Communications*, vol. 5, no. 1, p. 4006, 2014.

[14] K.-H. Lue, Y.-F. Wu, S.-H. Liu et al., "Prognostic value of pretreatment radiomic features of 18F-fdg PET in patients with Hodgkin lymphoma," *Clinical Nuclear Medicine*, vol. 44, no. 10, pp. e559–e565, 2019.

[15] K. Lue, Y. Wu, and H. Lin, "Prognostic value of baseline radiomic features of 18F-fdg PET in patients with diffuse large B-cell lymphoma," *Diagnostics*, vol. 11, no. 1, 2021.

[16] Y. Zhou, X.-L. Ma, L.-T. Pu, R.-F. Zhou, X.-J. Ou, and R. Tian, "Prediction of overall survival and progression-free survival by the 18F-fdg PET/CT radiomic features in patients with primary gastric diffuse large B-cell lymphoma," *Contrast Media and Molecular Imaging*, vol. 2019, pp. 1–9, 2019.

[17] M. E. Mayerhoefer, C. C. Riedl, A. Kumar et al., "Radiomic features of glucose metabolism enable prediction of outcome in mantle cell lymphoma," *European Journal of Nuclear Medicine and Molecular Imaging*, vol. 46, no. 13, pp. 2760–2769, 2019.

[18] F. Lucia, D. Visvikis, M.-C. Desseroit et al., "Prediction of outcome using pretreatment 18F-FDG PET/CT and MRI radiomics in locally advanced cervical cancer treated with chemoradiotherapy," *European Journal of Nuclear Medicine and Molecular Imaging*, vol. 45, no. 5, pp. 768–786, 2018.

[19] J. Zhao, W. Zhang, and Y. Zhu, "Development and validation of noninvasive MRI-based signature for preoperative prediction of early recurrence in perihilar cholangiocarcinoma," *Journal of Magnetic Resonance Imaging*, vol. 2021, 2021.

[20] C. Nioche, F. Orlhac, S. Boughdad et al., "LIFEx: a freeware for radiomic feature calculation in multimodality imaging to accelerate advances in the characterization of tumor heterogeneity," *Cancer Research*, vol. 78, no. 16, pp. 4786–4789, 2018.

[21] R. Boellaard, R. Delgado-Bolton, W. J. G. Oyen et al., "FDG PET/CT: EANM procedure guidelines for tumour imaging: version 2.0," *European Journal of Nuclear Medicine and Molecular Imaging*, vol. 42, no. 2, pp. 328–354, 2015.

[22] S. Ha, H. Choi, J. C. Paeng, and G. J. Cheon, "Radiomics in oncological PET/CT: a methodological overview," *Nuclear Medicine and Molecular Imaging*, vol. 53, no. 1, pp. 14–29, 2019.

[23] F. Orlhac, C. Nioche, M. Soussan, and I. Buvat, "Understanding changes in tumor texture indices in PET: a comparison between visual assessment and index values in simulated and patient data," *Journal of Nuclear Medicine*, vol. 58, no. 3, pp. 387–392, 2017.

[24] A. Zwanenburg, "Radiomics in nuclear medicine: robustness, reproducibility, standardization, and how to avoid data analysis traps and replication crisis," *European Journal of Nuclear Medicine and Molecular Imaging*, vol. 46, no. 13, pp. 2638–2655, 2019.

[25] A. K. Jha, S. Mithun, and V. Jaiswar, "Repeatability and reproducibility study of radiomic features on a phantom and human cohort," *Scientific Reports*, vol. 11, no. 1, p. 2021.

[26] R. T. H. Leijenaar, S. Carvalho, E. R. Velazquez et al., "Stability of FDG-PET Radiomics features: an integrated analysis of test-retest and inter-observer variability," *Acta Oncologica*, vol. 52, no. 7, pp. 1391–1397, 2013.

[27] R. Tibshirani, "The lasso method for variable selection in the Cox model," *Statistics in Medicine*, vol. 16, no. 4, pp. 385–395, 1997.

[28] B. Zhang, J. Tian, D. Dong et al., "Radiomics features of multiparametric MRI as novel prognostic factors in advanced nasopharyngeal carcinoma," *Clinical Cancer Research*, vol. 23, no. 15, pp. 4259–4269, 2017.

[29] F. Rotolo, J. P. Pignon, J. Bourhis et al., "Surrogate end points for overall survival in loco-regionally advanced nasopharyngeal carcinoma: an individual patient data meta-analysis," *Journal of the National Cancer Institute*, vol. 109, no. 4, 2017.

[30] K.-Y. Ko, C.-J. Liu, C.-L. Ko, and R.-F. Yen, "Intratumoral heterogeneity of pretreatment 18F-fdg PET images predict disease progression in patients with nasal type extranodal natural killer/T-cell lymphoma," *Clinical Nuclear Medicine*, vol. 41, no. 12, pp. 922–926, 2016.

[31] S. Araf, K. Korfi, F. Bewicke-Copley et al., "Genetic heterogeneity highlighted by differential FDG-PET response in diffuse large B-cell lymphoma," *Haematologica*, vol. 105, no. 6, pp. 318–321, 2020.

[32] N. McGranahan and C. Swanton, "Clonal heterogeneity and tumor evolution: past, present, and the future," *Cell*, vol. 168, no. 4, pp. 613–628, 2017.

[33] G. Stanta and S. Bonin, "Overview on clinical relevance of intra-tumor heterogeneity," *Frontiers of Medicine*, vol. 5, p. 85, 2018.

[34] P. Lambin, E. Rios-Velazquez, R. Leijenaar et al., "Radiomics: extracting more information from medical images using advanced feature analysis," *European Journal of Cancer*, vol. 48, no. 4, pp. 441–446, 2012.

[35] N.-M. Cheng, Y.-H. D. Fang, L.-y. Lee et al., "Zone-size nonuniformity of 18F-FDG PET regional textural features predicts survival in patients with oropharyngeal cancer," *European Journal of Nuclear Medicine and Molecular Imaging*, vol. 42, no. 3, pp. 419–428, 2015.

[36] H. Lee, D.-e. Lee, S. Park et al., "Predicting response to neoadjuvant chemotherapy in patients with breast cancer," *Clinical Nuclear Medicine*, vol. 44, no. 1, pp. 21–29, 2019.

[37] Y. Hu, X. Zhao, J. Zhang, J. Han, and M. Dai, "Value of 18F-FDG PET/CT radiomic features to distinguish solitary lung adenocarcinoma from tuberculosis," *European Journal of Nuclear Medicine and Molecular Imaging*, vol. 48, no. 1, pp. 231–240, 2021.

[38] K.-H. Lue, Y.-F. Wu, S.-H. Liu et al., "Intratumor heterogeneity assessed by 18F-fdg PET/CT predicts treatment response and survival outcomes in patients with Hodgkin lymphoma," *Academic Radiology*, vol. 27, no. 8, pp. e183–e192, 2020.

[39] A.-S. Cottereau, A. Versari, A. Loft et al., "Prognostic value of baseline metabolic tumor volume in early-stage Hodgkin lymphoma in the standard arm of the H10 trial," *Blood*, vol. 131, no. 13, pp. 1456–1463, 2018.

[40] D. Albano, A. Mazzoletti, M. Spallino et al., "Prognostic role of baseline 18F-FDG PET/CT metabolic parameters in elderly HL: a two-center experience in 123 patients," *Annals of Hematology*, vol. 99, no. 6, pp. 1321–1330, 2020.

[41] A. Parvez, N. Tau, D. Hussey, M. Maganti, and U. Metser, "18F-FDG PET/CT metabolic tumor parameters and radiomics features in aggressive non-Hodgkin's lymphoma as predictors of treatment outcome and survival," *Annals of Nuclear Medicine*, vol. 32, no. 6, pp. 410–416, 2018.

[42] S.-C. Chan, K.-P. Chang, Y.-H. D. Fang et al., "Tumor heterogeneity measured on F-18 fluorodeoxyglucose positron emission tomography/computed tomography combined with plasma Epstein-Barr Virus load predicts prognosis in patients with primary nasopharyngeal carcinoma," *The Laryngoscope*, vol. 127, no. 1, pp. E22–E28, 2017.

[43] Y. Jiang, Q. Yuan, W. Lv et al., "Radiomic signature of 18F fluorodeoxyglucose PET/CT for prediction of gastric cancer survival and chemotherapeutic benefits," *Theranostics*, vol. 8, no. 21, pp. 5915–5928, 2018.

[44] R. T. H. Leijenaar, S. Carvalho, E. R. Velazquez et al., "Stability of FDG-PET radiomics features: an integrated analysis of test-retest and inter-observer variability," *Acta Oncologica*, vol. 52, no. 7, pp. 1391–1397, 2013.

[45] M. Vallières, A. Zwanenburg, B. Badic, C. Cheze Le Rest, D. Visvikis, and M. Hatt, "Responsible radiomics research for faster clinical translation," *Journal of Nuclear Medicine Official Publicatio, Society of Nuclear Medicine*, vol. 59, no. 2, pp. 189–193, 2018.

[46] L. Lu, W. Lv, J. Jiang et al., "Robustness of radiomic features in [11C]choline and [18F]FDG PET/CT imaging of nasopharyngeal carcinoma: impact of segmentation and discretization," *Molecular Imaging and Biology*, vol. 18, no. 6, pp. 935–945, 2016.